

MEASURING LONG-DISTANCES IN ¹⁵N SELECTIVELY AMINO ACID LABELED PROTEINS USING NUCLEAR MAGNETIC RESONANCE (NMR) SPECTROSCOPY

Jake Simmons* and Matthew D. Shannon†

Department of Chemistry and Biochemistry, Stetson University, Deland, FL 32723

Abstract

Paramagnetic ions can be used as atomic rulers in NMR spectroscopy to probe long distances in proteins. To expand the capability of this methodology, a uniformly ¹⁵N-labeled K28H GB1 protein and a ¹⁵N phenylalanine (F) K28H GB1 selectively labeled protein were expressed and purified. Herein, it is shown that Cu²⁺ strongly chelates to a mutated solvent-exposed histidine residue in both samples in the presence of a ligand, nitrilotriacetic acid (NTA). 2-D ¹H-¹⁵N HSQC spectra using the ¹⁵N uniformly labeled sample and 1-D ¹H ¹⁵N-filtered spectra using the ¹⁵N F labeled sample were recorded on both the diamagnetic sample (no Cu²⁺) and the paramagnetic Cu²⁺ sample to extract paramagnetic relaxation enhancements (PREs). The PREs were easily converted into distances, which were in semi-quantitative agreement with the known distances. Ultimately, ¹⁵N-specific amino acid labeling demonstrates value for large proteins or intrinsically disordered proteins with lots of peak overlap in 2-D spectra.

†Corresponding author: mshannon1@stetson.edu

*Undergraduate researcher and co-author

Keywords: NMR, PRE, ¹⁵N-labeling, Cu²⁺, protein structure, mutagenesis

Received: May 22, 2023

Accepted: June 2, 2023

Published: June 13, 2023

Introduction

Nuclear Magnetic Spectroscopy (NMR) is a widely used spectroscopic technique to probe the structure and dynamics of macromolecules. Advances in both technology and methodology have driven its rise over the last few decades as a competitor to X-ray crystallography and more recently, cryo-EM, in the field of structural biology. Since NMR samples mimic their physiological condition and do not require crystallization or rapid freeze treatment, NMR is the preferred method for samples that aim to mimic *in vivo* conditions and/or for samples used to measure protein dynamics.¹ NMR has benefited recently from increases in magnetic field strength and cryoprobe innovation, which have greatly increased both the sensitivity and resolution of experiments. Also, methodological advancements in NMR have occurred including improvements in sample preparation, pulse sequences, and experimental design/theory.² Herein, a methodological application will be demonstrated on a model, small protein GB1 that combines the well-established paramagnetic relaxation enhancement (PRE) method on a ¹⁵N-amino acid specifically labeled sample.

PREs are measurable NMR parameters that are used to extract long-range distances (1-3 nm) using the Solomon equations on paramagnetic protein samples that have isotropic magnetic susceptibility.³ The measurement of long distances in NMR has proven to be extremely useful for *de novo* protein structure determination and to improve the resolution of structures.⁴⁻⁸ Since most proteins are natively diamagnetic, a paramagnetic center such as a nitroxide label or Cu²⁺ must be introduced as a site-specific tag.⁸ To measure PREs (longitudinal or transverse), relaxation rates must be measured and compared in both the diamagnetic (control) and paramagnetic samples. Qualitatively, if no difference in relaxation is observed for a unique NMR peak (e.g., ¹H-¹⁵N pair in an amino acid), then that amino acid is “far” from the paramagnetic center. On the other hand, if a significant difference in relaxation rate is observed, then that amino acid is “close” to the paramagnetic center (Figure 1).

To quantify PREs, an experimental PRE must first be measured with high precision and converted into distance using theory

based on the Solomon equations.³ In this work, ¹H transverse PREs are measured. To experimentally determine ¹H transverse PREs using a 2-point estimate, the peak volume ratio between a paramagnetic and diamagnetic sample can be measured for each peak by recording a 2-D ¹H-¹⁵N HSQC experiment.⁹ Since peak volume is proportional to the line broadening, or the ¹H transverse relaxation rate, the experimentally measured ¹H transverse PRE can be determined by the following (two-point time estimate):

$$\text{Equation 1: Transverse PRE} = \Gamma_2(\text{Hz}) = R_2(\text{para}) - R_2(\text{dia}) = -\frac{1 \ln\left(\frac{V_{\text{para}}}{V_{\text{dia}}}\right)}{2 \times 0.00526}$$

where 0.00526 seconds = 1/(2(J_{NH})) and R₂ = 1/T₂ (reciprocal of transverse relaxation time).

To convert the experimentally measure ¹H transverse PREs into a distance, the following equation can be used:³

$$\text{Equation 2: } \Gamma_2(\text{Hz}) = \frac{1}{15} * \left(\frac{\mu_0}{4\pi}\right)^2 * \gamma^2 * g^2 * \mu_B^2 * S(S+1) * r^{-6} * \left(4\lambda_c + \frac{3\lambda_c}{1+(\omega_H\lambda_c)^2}\right),$$

where r is the distance between the unpaired electron and nucleus, S = ½ for Cu²⁺, and λ_c is the correlation time for the electron-nucleus dipolar coupling (2.5 ns for Cu²⁺).¹⁰




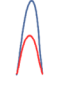


Diamagnetic vs. Paramagnetic		V _{para} /V _{dia} or A _{para} /A _{dia}	¹ H Transverse PRE	Distance
2D	1D			
		1	0	> 2 nm
		0.5	64	~ 1.2 nm
		~ 0	> 500 (very large)	< 1 nm (very close)

Figure 1: Illustration of ¹H transverse PRE effects with Cu²⁺ on NMR peaks at various distances. Expected 2-D and 1-D NMR peak volume and area changes respectively are illustrated in a diamagnetic (no Cu²⁺) and a paramagnetic sample (Cu²⁺) when the paramagnetic metal is “far” away from an amino acid (top row), is at an intermediate distance from an amino acid (middle row), or is “close” to an amino acid (bottom row).

Simulations of the above equations are shown in **Figure 2**. If an HSQC experiment is conducted on both the diamagnetic and paramagnetic sample, a PRE is measured using **equation 1**. The experimentally measured PRE can easily be converted into a distance using **equation 2** as shown in **Figure 2**.

Since transverse ^1H PREs commonly rely on high resolution in 2-D NMR, the data analysis can be time-consuming but also impossible for amino acid peaks that exhibit peak overlap. Peak overlap is extremely common in large proteins due to a large number of amino acid peaks and intrinsically disordered proteins (IDPs) that suffer from poor chemical shift dispersion. To alleviate this bottleneck, ^{15}N -amino acid specific labeling can be employed.¹¹ This severely reduces the number of peaks in 2-D spectra and possibly allows for 1-D ^{15}N -filtered ^1H -detected spectra to be recorded to measure the PREs. Herein, ^{15}N phenylalanine (“F”) labeling is used on a GB1 protein, a model well-studied protein for NMR methods, to demonstrate that 1-D ^1H NMR spectra (^{15}N -filtered) can be used to measure ^1H transverse PREs using a rigid Cu^{2+} binding motif with moderate precision and accuracy in a straightforward manner.

MATERIAL AND METHODS

Construction of K28H GB1 plasmids

Site-directed mutagenesis (SDM) was carried out to mutate a solvent-exposed lysine to a histidine residue at the 28th position (“K28H”) in the GB1 pet11a plasmid. To perform this mutation, a forward and reverse primer were designed using PrimerX (<https://www.bioinformatics.org/primerx/>). The following primers were then ordered from Integrated DNA Technologies:

Forward: 5' CGCTGCTACCGCGGAACATGTTTTCAAACAGTACGC 3'

Reverse: 5' GCGTACTGTTTGAAAACATGTTCCGCGGTAGCAGCG 3'

A set of eight 25 μL polymerase chain reactions (PCR) were carried out as shown in **Table 1**. After preparing the eight samples, the heat cycle shown in **Table 2** was used to conduct the eight PCR reactions.

A 1% agarose gel was run on all eight tubes to screen for successful PCR products. Potential products were digested with 1 μL

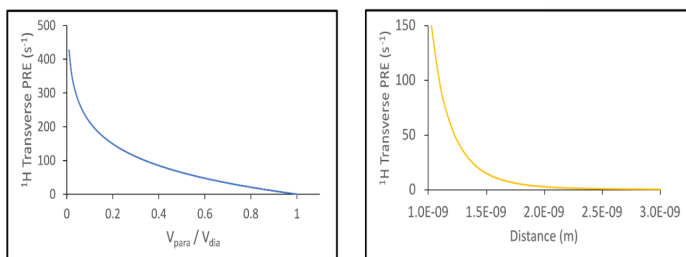


Figure 2: Experimentally measured and theoretically predicted ^1H transverse PREs. Using equation 1, ^1H transverse PREs are simulated as a function of the paramagnetic: diamagnetic peak volume/area ratio (left). Using equation 2, ^1H transverse PREs are simulated for Cu^{2+} as a function of distance. By recording a paramagnetic and diamagnetic spectrum on a sample, experimental PREs can be determined using the simulation of the left. These PREs are easily converted into distances using the simulation on the right.

of DpnI to remove unwanted methylated DNA products. The DpnI digested PCR products were then transformed into DH5 α competent cells and plated on ampicillin-resistant LB-agar plates. Single colonies were selected and mini-prepped (Qiagen mini-prep kits) for DNA sequencing. The successful incorporation of the mutation was confirmed by DNA sequencing (T7 promoter).

Expression and Purification of ^{15}N -labeled GB1 samples

The K28H GB1 pet11a plasmid was transformed (~ 10 ng) into *E. coli* BL21(DE3) competent cells and plated on ampicillin-resistant LB-agar plates. A single colony was selected and grown in 2 mL of LB-ampicillin media. After ~ 8 hours, 150 μL of this saturated culture was transferred into a 25 mL overnight minimal media (ampicillin resistant) with 1 mg/mL of $^{15}\text{NH}_4\text{Cl}$ as the sole nitrogen source to generate a uniformly ^{15}N -labeled sample.¹² The saturated overnight culture was then transferred into a 500 mL minimal media (1 mg/mL $^{15}\text{NH}_4\text{Cl}$) culture. This culture was grown until the $\text{OD}_{600\text{nm}}$ reached ~ 0.6 . At this point, IPTG was added to a final concentration of 0.5 mM to induce protein expression. After four hours, the cells were pelleted by centrifugation at 4,000 $\times g$ for 20 minutes at 4°C. To prepare a ^{15}N -F specifically labeled sample, the same protocol was used except all 20 amino acids were used as the nitrogen source in which the phenylalanine (“F”) was ^{15}N -labeled. The amounts and concentrations used varied and were based on work by Traaseth *et al.*¹³ To purify both ^{15}N -K28H GB1 samples, the pellets were resuspended in “lysis” buffer (50 mM Tris-HCl pH 8, 300 mM NaCl). The samples were then purified by cell lysis, a heat purification step at 80°C, and by size-exclusion chromatography (HiPrep 16/60 Sephacryl S-100 HR) as described previously.¹⁴ The fractions containing pure protein were then combined and concentrated in MES buffer (pH 6.5).

NMR Spectroscopy and Data Analysis

The uniformly labeled ^{15}N sample and the ^{15}N -F specifically labeled sample had final concentrations of ~ 1.5 mM and ~ 1.15 mM respectively in pH 6.5 MES buffer (10% $\text{D}_2\text{O}/90\%$ H_2O) for NMR experiments. All NMR experiments were recorded on a diamagnetic (no Cu^{2+}) and a paramagnetic sample with nitrioloacetic acid (NTA) and Cu^{2+} at various amounts.

All NMR data were obtained on a JEOL 400 MHz spectrometer at 298K using a double resonance probe tuned to ^1H and ^{15}N . 1-D ^{15}N -filtered ^1H -detected HSQC experiments were recorded in ~ 10 minutes on the ^{15}N -F sample and 2-D HSQC (^1H - ^{15}N) experi-

Table 1. PCR reaction conditions using Q5 Master Mix:

Reagent	Volume (μL)	Final Concentration/Amount
Q5 2X Master Mix	12.5	1X
10 μM Forward primer	1.25	0.5 μM
10 μM Reverse primer	1.25	0.5 μM
10 ng/ μL plasmid	1	10 ng
Nuclease-free water	9	

Table 2. Thermocycler conditions used for PCR reactions

Initial Denaturation	98°C	30 sec
30 Cycles	98°C	10 seconds
	54-66°C (gradient – 8 tubes)	30 seconds
	72°C	6 minutes
Final extension	72°C	2 minutes
Hold	4°C	Indefinitely

ments were recorded in ~ 30 minutes on the ^{15}N -uniformly labeled sample.

Once the NMR experiments were completed, the 1-D data sets were processed and analyzed using JEOL Delta NMR software. The peak areas were exported for the paramagnetic and diamagnetic samples to calculate the PREs. The 2-D data sets were converted to NMRPipe¹⁵ for processing. Peak volumes were extracted using the peak detection tool, and the peak volumes of the paramagnetic and diamagnetic samples were extracted. To calculate the ^1H transverse PREs, **equation 1** was used (2-point estimate).⁹ Using **equation 2**, the ^1H transverse PREs were converted into distances. The 2-D data was also converted to Sparky¹⁶ for visualization to display overlays of the paramagnetic and diamagnetic data.

RESULTS

Initially, to characterize both ^{15}N -labeled samples, 2-D HSQC experiments were recorded and analyzed. In **Figure 3**, an overlay of the ^{15}N -F sample is shown on top of the uniformly labeled ^{15}N sample. Each peak in the 2-D HSQC of the ^{15}N uniformly labeled sample can be assigned to a backbone N-H pair of each amino acid based on previous work,¹⁷ which confirmed that the protein was properly folded upon the mutation. In addition, the ^{15}N -F sample clearly only had two peaks present in the 2-D HSQC, which confirms that no ^{15}N -labeling “scrambling” occurred since only the two phenylalanine residues were ^{15}N -labeled during the expression. Interestingly, the F30 residue and the Y45 residue are overlapped in the 2-D HSQC of the ^{15}N -uniformly labeled sample. This demonstrates that ^{15}N -amino acid labeling is a powerful tool when peak overlap is an issue in larger proteins or IDPs.

It is proposed that Cu^{2+} in the presence of an external ligand such as IDA or NTA chelates to a solvent-exposed histidine, which forms an octahedral complex with Cu^{2+} as shown in **Figure 6A**.¹⁸ To confirm this, a titration was first performed on the ^{15}N -uniformly labeled sample to ensure that Cu^{2+} specifically bound to the mutated histidine residue. In **Figure 4**, a 2-D overlay of the paramagnetic spectrum with an equimolar ratio of Cu^{2+} :protein is shown

on top of the diamagnetic control spectrum. This overlay shows that amino acids closest to H28 (H28, V29, and K31) exhibited extremely strong PRE's ($\gg 150$) and are therefore calculated to be less than 1 nm from the bound Cu^{2+} . Some amino acids slightly farther away from H28 exhibited intermediate broadening (T25, E27, and A34), and therefore their distances are quantified as 1.20, 1.25, and 1.50 nm respectively based on **equations 1 and 2** compared to their predicted distance (pdb: 1pga) of 0.75, 0.75, and 1.05 nm respectively. The experimental and predicted distances are in reasonable agreement, and their discrepancies are addressed further in the discussion. Interestingly, there is evidence that F30 experienced intermediate broadening as well; however, it is overlapped by Y45 in the 2-D spectrum marked by an asterisk. Even at equimolar ratios of Cu^{2+} :protein, it is evident that the Cu^{2+} has a specific, strong affinity for K28H compared to any other potential secondary binding sites such as a glutamate or aspartate, which could also chelate to Cu^{2+} .

To assess the possibility of ^1H transverse PRE measurements on the ^{15}N -F specially labeled sample, a Cu^{2+} /NTA:protein titration was also performed on this sample at various amounts. Since F30 and F52 are the only ^{15}N -labeled amino acids in the entire protein, a 1-D ^1H NMR experiment was recorded that was filtered through ^{15}N (“out and back”) using the same pulse sequence to generate the 2-D HSQC spectra. As shown in **Figure 5**, F52 exhibits no change in its peak area within noise upon addition of Cu^{2+} since it is far in space from K28H. This was promising as peaks far away in space (~ 2 nm or more) are expected to have no ^1H transverse PRE (**Figure 2B**). On the other hand, F30 exhibited relatively strong PREs that increased as the Cu^{2+} amount increased as expected since F30 is close to K28H in 3-D space. Since the peak did not completely broaden, or disappear, its ^1H transverse PRE was calculated using the peak area (or integration number) ratio between the diamagnetic and paramagnetic sample as shown in **equation 1**. The ^1H transverse PRE was then converted into a distance using **equation 2**. The experimentally calculated distance was then compared to the predicted distance based on the known structure of GB1. Since the histidine at position 28 is solvent-exposed and presumably flexi-

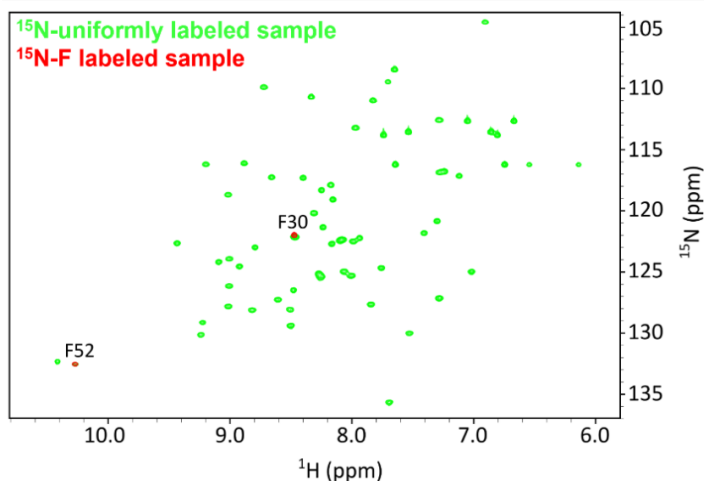


Figure 3: Initial 2-D HSQC of ^{15}N -labeled K28H GB1 diamagnetic samples. An overlay using Sparky of the purified ^{15}N -F labeled K28H GB1 protein on top of the purified ^{15}N -uniformly labeled K28H protein. The two phenylalanine peaks, F30 and F52, are labeled. The assignments of all the peaks are known based on previous assignments made (note F30 and Y45 are overlapped in the uniformly labeled sample).

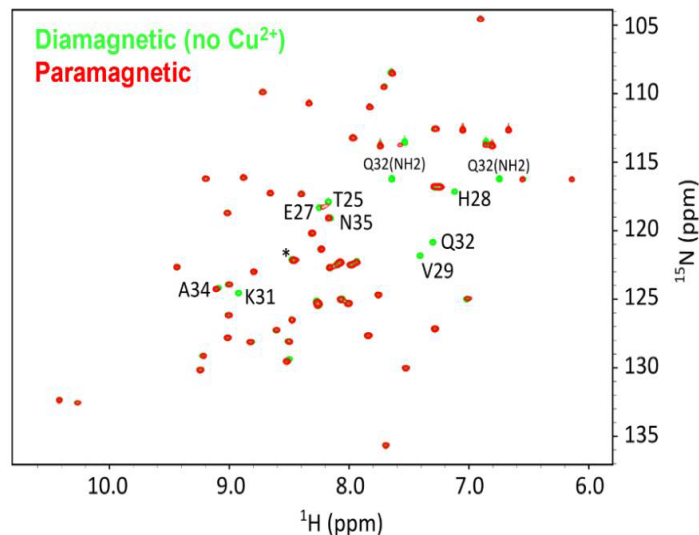


Figure 4: Overlay of the paramagnetic and diamagnetic K28H ^{15}N -uniformly GB1 labeled samples. An overlay using Sparky of the paramagnetic sample with Cu^{2+} on top of the diamagnetic reference sample. Unsurprisingly, amino acids near the K28H Cu^{2+} binding site are either partially or completely broadened out, which demonstrates that Cu^{2+} is strongly binding to that site only.

ble, a range of sidechain histidine imine N to backbone F30/F52 amide distances were estimated in PyMol (**Table 3**).¹⁹ Again, the ¹⁵N-F experimental distances display reasonable agreement with the predicted distances since proper distance trends (F30 is much closer than F52) are observed. The precision of the data and distance discrepancies are addressed in the discussion.

DISCUSSION

In summary, it has been shown that semi-quantitative long distances can be estimated in an efficient, straightforward way (1-D ¹H NMR) by combining ¹⁵N-specific amino acid labeling with PREs. In general, a set of measured distances can aid in the structure determination of macromolecules, as well as to resolve site-specific intermolecular contacts. The bottleneck of this work instead becomes sample preparation and not the analysis of NMR data with an abundance of peak overlap. The data is straightforward to acquire and analyze, which makes it a promising method for large proteins or IDPs that have a lot of peak overlap in 2-D HSQC spectra, especially at lower magnetic fields that suffer from lower resolution. Samples that are ¹⁵N-specifically amino acid labeled can also be used to measure site-specific dynamics at those labeled sites, which may be inaccessible otherwise due to peak overlap.

As shown in **Table 3**, the experimentally measured distances are slight overestimates; however, it is likely that the Cu²⁺ is far-

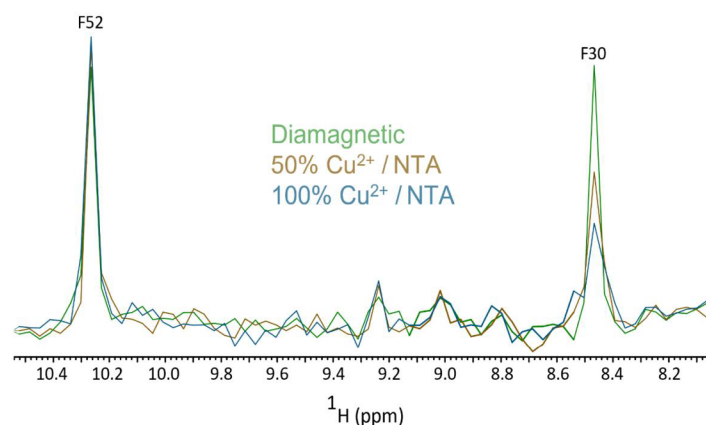


Figure 5: Overlay of the paramagnetic and diamagnetic K28H ¹⁵N-F GB1 labeled samples. 1-D ¹H NMR ¹⁵N-filtered spectra are shown for the diamagnetic reference sample and two paramagnetic samples at submolar (50%) and equimolar (100%) amounts of Cu²⁺. By taking the peak area ratio (integration number ratio) between the paramagnetic and diamagnetic sample for the F30 peak, PREs and therefore distances were calculated using this data. Note that no PRE was observed (i.e., no change in peak area) for F52 as it was too “far” away from the paramagnetic metal.

Table 3: Comparing predicted and experimentally determined distances to F30/F52. The measured distances were calculated from the experimentally measured PREs from the 1-D data set. The estimated distances were determined by measuring the imine histidine nitrogen to backbone amide nitrogen distances in PyMol from a series of seven generated K28H conformations (pdb 1pga).²¹

Amino Acid	Measured distance from Cu ²⁺ to backbone nitrogen (Å)	Estimated distances from imine nitrogen to backbone nitrogen using seven 28H Conformations (Å)
F30	~ 11.5	5.8 – 8.1
F52	> ~ 15 *	12.4 – 15.6

*No PRE was detected so a minimum distance of 15 Å can be assumed within experimental noise

ther away in 3-D space than the imine nitrogen on histidine due to steric hindrance caused by nearby sidechains. This would shift the estimated distances up approximately two angstroms, which would alleviate some of the error, since two slightly different measurements are technically compared. Another potential concern is that the distance measured experimentally is a population-weighted average distance of multiple sidechain histidine conformations that may result in mediocre precision. This potential concern is illustrated in **Figure 6** as it is suspected that the histidine-Cu²⁺ binding is flexible in a range of conformational space. To overcome the lack of precision in the data, a double histidine mutation can be prepared to rigidify the location of the paramagnetic Cu²⁺ between two histidine residues in the presence of NTA.²⁰ To do this, SDM can be carried out to insert another solvent-exposed histidine 4 residues apart on an alpha helix or 2 residues apart on a beta sheet. For example, a K28H/Q32H double histidine GB1 mutation could be constructed along the alpha-helix. The double histidine motif has successfully been demonstrated in electron paramagnetic resonance (EPR) experiments to increase the precision of long-distance measurements.²⁰ Additionally, future work using this methodology on different metals that have a higher spin (S) such as Mn²⁺ will also be investigated to probe longer distances (2-3 nm) since the PRE effects become even stronger.

ACKNOWLEDGEMENTS

The authors want to thank Stetson University for the generous start-up funds and a summer grant to support this work. We also want to thank the Department of Chemistry and Biochemistry for their thoughtful advice and support of this work.

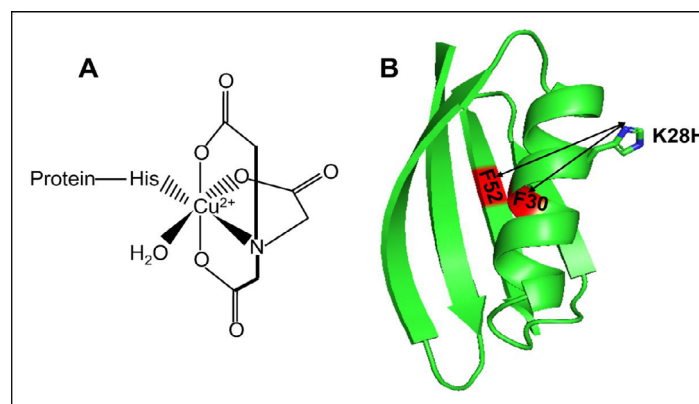


Figure 6: Illustration of Cu²⁺ binding to histidine in the presence of NTA. (A) Depiction of the octahedral Cu²⁺ binding motif to histidine in the presence of NTA. (B) Distance predictions from the histidine imine N to each backbone amide phenylalanine (F30 or F52) using one of the histidine (K28H) orientations in PyMol (pdb: 1pga).²¹

REFERENCES

- (1). Hu, Y.; Cheng, K.; He, L.; Zhang, X.; Jiang, B.; Jiang, L.; Li, C.; Wang, G.; Yang, Y.; Liu, M. NMR-Based Methods for Protein Analysis. *Anal. Chem.* **2021**, *93* (4).
- (2). Arthanari, H.; Takeuchi, K.; Dubey, A.; Wagner, G. Emerging Solution NMR Methods to Illuminate the Structural and Dynamic Properties of Proteins. *Current Opinion in Structural Biology.* **2019**, *58*.
- (3). Solomon, I. Relaxation processes in a system of two spins.

- Phys. Rev.*, **1955**, 99 (2).
- (4). Gillespie, J. R.; Shortle, D. Characterization of Long-Range Structure in the Denatured State of Staphylococcal Nuclease. I. Paramagnetic Relaxation Enhancement by Nitroxide Spin Labels. *J. Mol. Biol.* **1997**, 268 (1).
- (5). Battiste, J. L.; Wagner, G. Utilization of Site-Directed Spin Labeling and High-Resolution Heteronuclear Nuclear Magnetic Resonance for Global Fold Determination of Large Proteins with Limited Nuclear Overhauser Effect Data. *Biochemistry* **2000**, 39 (18).
- (6). Donaldson, L. W.; Skrynnikov, N. R.; Choy, W. Y.; Muhandiram, D. R.; Sarkar, B.; Forman-Kay, J. D.; Kay, L. E. Structural Characterization of Proteins with an Attached ATCUN Motif by Paramagnetic Relaxation Enhancement NMR Spectroscopy. *J. Am. Chem. Soc.* **2001**, 123 (40).
- (7). Pintacuda, G.; Moshref, A.; Leonchiks, A.; Sharipo, A.; Otting, G. Site-Specific Labelling with a Metal Chelator for Protein-Structure Refinement. *J. Biomol. NMR* **2004**, 29 (3).
- (8). Otting, G. Protein NMR Using Paramagnetic Ions. *Annual Review of Biophysics*. **2010**, 39 (1).
- (9). Iwahara, J.; Tang, C.; Marius Clore, G. Practical Aspects of ¹H Transverse Paramagnetic Relaxation Enhancement Measurements on Macromolecules. *J. Magn. Reson.* **2007**, 184 (2).
- (10). Bertini, I.; Luchinat, C.; Giacomo, P. *Solution NMR of Paramagnetic Molecules: Applications to Metallobiomolecules and Models*; **2001**.
- (11). Muchmore, D. C.; McIntosh, L. P.; Russell, C. B.; Anderson, D. E.; Dahlquist, F. W. Expression and Nitrogen-15 Labeling of Proteins for Proton and Nitrogen-15 Nuclear Magnetic Resonance. *Methods Enzymol.* **1989**, 177 (C).
- (12). Cai, M.; Huang, Y.; Sakaguchi, K.; Clore, G. M.; Gronenborn, A. M.; Craigie, R. An Efficient and Cost-Effective Isotope Labeling Protocol for Proteins Expressed in Escherichia Coli. *J. Biomol. NMR* **1998**, 11 (1).
- (13). Gayen, A.; Banigan, J. R.; Traaseth, N. J. Ligand-Induced Conformational Changes of the Multidrug Resistance Transporter EmrE Probed by Oriented Solid-State NMR Spectroscopy. *Angew. Chemie - Int. Ed.* **2013**, 52 (39).
- (14). Franks, W. T.; Zhou, D. H.; Wylie, B. J.; Money, B. G.; Graesser, D. T.; Frericks, H. L.; Sahota, G.; Rienstra, C. M. Magic-Angle Spinning Solid-State NMR Spectroscopy of the B1 Immunoglobulin Binding Domain of Protein G (GB1): ¹⁵N and ¹³C Chemical Shift Assignments and Conformational Analysis. *J. Am. Chem. Soc.* **2005**, 127 (35).
- (15). Delaglio, F.; Grzesiek, S.; Vuister, G. W.; Zhu, G.; Pfeifer, J.; Bax, A. NMRPipe: A Multidimensional Spectral Processing System Based on UNIX Pipes. *J. Biomol. NMR* **1995**, 6 (3).
- (16). Goddard, Td.; Kneller, D. G. Sparky 3. *Univ. California, San Fr.* **2004**, 14.
- (17). Gronenborn, A. M.; Filpula, D. R.; Essig, N. Z.; Achari, A.; Whitlow, M.; Wingfield, P. T.; Clore, G. M. A Novel, Highly Stable Fold of the Immunoglobulin Binding Domain of Streptococcal Protein G. *Science* **1991**.
- (18). Nomura, M.; Kobayashi, T.; Kohno, T.; Fujiwara, K.; Tenno, T.; Shirakawa, M.; Ishizaki, I.; Yamamoto, K.; Matsuyama, T.; Mishima, M.; Kojima, C. Paramagnetic NMR Study of Cu²⁺-IDA Complex Localization on a Protein Surface and Its Application to Elucidate Long Distance Information. *FEBS Lett.* **2004**.
- (19). Delano, W. L. The PyMOL Molecular Graphics System. *CCP4 Newsl. protein Crystallogr.* **2002**, 40 (1).
- (20). Cunningham, T. F.; Putterman, M. R.; Desai, A.; Horne, W. S.; Saxena, S. The Double-Histidine Cu²⁺-Binding Motif: A Highly Rigid, Site-Specific Spin Probe for Electron Spin Resonance Distance Measurements. *Angew. Chemie - Int. Ed.* **2015**, 54 (21).
- (21). Gallagher, T.; Alexander, P.; Bryan, P.; Gilliland, G. L. Two Crystal Structures of the B1 Immunoglobulin-Binding Domain of Streptococcal Protein G and Comparison with NMR. *Biochemistry* **1994**, 33 (15).